

Calcium-Dependent Assembly of Centrin–G-Protein Complex in Photoreceptor Cells

Alexander Pulvermüller,^{1*} Andreas Gieβl,² Martin Heck,¹ Ralf Wottrich,^{2†} Angelika Schmitt,²
Oliver Peter Ernst,¹ Hui-Woog Choe,^{1,3} Klaus Peter Hofmann,¹ and Uwe Wolfrum^{2*}

*Institut für Medizinische Physik und Biophysik, Humboldt-Universität zu Berlin, Universitätsklinikum Charité, 10098 Berlin,¹
and Institut für Zoologie, Johannes Gutenberg-Universität Mainz, 55099 Mainz,² Germany, and
Department of Chemistry, Chonbuk National University, Chonju, South Korea³*

Received 25 June 2001/Returned for modification 3 August 2001/Accepted 17 December 2001

Photoexcitation of rhodopsin activates a heterotrimeric G-protein cascade leading to cyclic GMP hydrolysis in vertebrate photoreceptors. Light-induced exchanges of the visual G-protein transducin between the outer and inner segment of rod photoreceptors occur through the narrow connecting cilium. Here we demonstrate that transducin colocalizes with the Ca²⁺-binding protein centrin 1 in a specific domain of this cilium. Coimmunoprecipitation, centrifugation, centrin overlay, size exclusion chromatography, and kinetic light-scattering experiments indicate that Ca²⁺-activated centrin 1 binds with high affinity and specificity to transducin. The assembly of centrin–G-protein complex is mediated by the βγ-complex. The Ca²⁺-dependent assembly of a G protein with centrin is a novel aspect of the supply of signaling proteins in sensory cells and a potential link between molecular translocations and signal transduction in general.

Vertebrate photoreceptor cells are highly polarized neurons which consist of morphologically and functionally distinct cellular compartments (Fig. 1A). In both rod and cone photoreceptors, the light-sensitive photoreceptor outer segment is linked with an inner segment and the cell body via a nonmotile cilium, the so-called connecting cilium. In both cell types, the outer segment contains all components of the visual transduction cascade, which in rods is arranged separate from the plasma membrane at hundreds of stacked membrane disks. Photoexcitation of the visual pigment rhodopsin activates a heterotrimeric G-protein (composed of an α-subunit bearing the guanine nucleotide binding site and an undissociable βγ-complex) cascade, leading to cyclic GMP (cGMP) hydrolysis in the cytoplasm and closing of cGMP-gated channels in the plasma membrane (19, 34, 37, 42).

Established roles of calcium ions in signal transduction include the restoration of the dark level of cGMP through Ca²⁺-dependent guanylate cyclase-activating proteins and mechanisms that are thought to act at the level of the activated receptor (34). Here we describe a fundamentally different role of Ca²⁺, namely, in the regulation of transducin transport and supply. Highly regulated cellular trafficking mechanisms (9, 29, 41, 55) mediate all intracellular exchanges between the inner segment and the outer segment through the slender cilium, the only cellular bridge between both segments. Rhodopsin is

translocated (5) via the ciliary membrane, and membrane-associated motor proteins (e.g., myosin VIIa and kinesin II) participate in ciliary transport (27, 30, 61, 62). Cytoskeletal molecules associated with ciliary translocation of transduction proteins have not yet been identified.

Besides the classical cytoskeleton of eukaryotic cells, nanofilaments have been identified and summarized as a fourth group of cytoskeletal elements in eukaryotes (4). These super-fine filaments are composed of several heterogeneous components, including centrans. Centrans, also known as caltractins, are members of a highly conserved subgroup of the EF-hand superfamily of Ca²⁺-binding proteins (46, 51). The first centrin was discovered as the major component of striated flagellar rootlets in unicellular green algae, where it participates in Ca²⁺-dependent and ATP-independent rootlet contractions (47). In mammals centrin proteins are ubiquitously expressed and commonly associated with centrosome-related structures such as spindle poles of dividing cells or centrioles in centrosomes and basal bodies (46, 51). In vertebrate photoreceptor cells, centrin is also localized at the basal body at the base of the connecting cilium, but furthermore, it is a prominent component in the connecting cilium (59, 60). Three centrin genes have been identified so far in mammals (14, 26, 33). While recent immunoelectron microscopy on human ciliated epithelial cells has nicely shown that the isoform centrin 3 is exclusively a core component of the basal body centriole (25), the centrin isoforms centrin 1 and centrin 2 are closely related and cannot be distinguished using polyclonal and monoclonal antibodies (25, 60). However, comparative reverse transcription-PCR experiments using isoform-specific primers demonstrate that centrin 2 is ubiquitously expressed, whereas centrin 1 expression is restricted to ciliated cells such as retinal photoreceptor cells (25, 60). This indicates that, in photoreceptor cilia, the centrin 1 isoform might function as a Ca²⁺-modulated cytoskeletal protein.

In this work, we provide several lines of evidence indicating

* Corresponding author. Mailing address for Alexander Pulvermüller: Institut für Medizinische Physik und Biophysik, Charité, Medizinische Fakultät der Humboldt-Universität zu Berlin, Ziegelstrasse 5-9, D-10117 Berlin, Germany. Phone: 49 (0)30 450 524176. Fax: 49 (0)30 450 524952. E-mail: alexander.pulvermueller@charite.de. Mailing address for Uwe Wolfrum: Institut für Zoologie, Abt. 1, Johannes Gutenberg-Universität Mainz, Müllerweg 6, D-55099 Mainz, Germany. Phone: 49 (0)6131 39 25148. Fax: 49 (0)6131 39 23815. E-mail: wolfrum@mail.uni-mainz.de.

† Present address: ITOX, Forschungszentrum Karlsruhe, 76128 Karlsruhe, Germany.

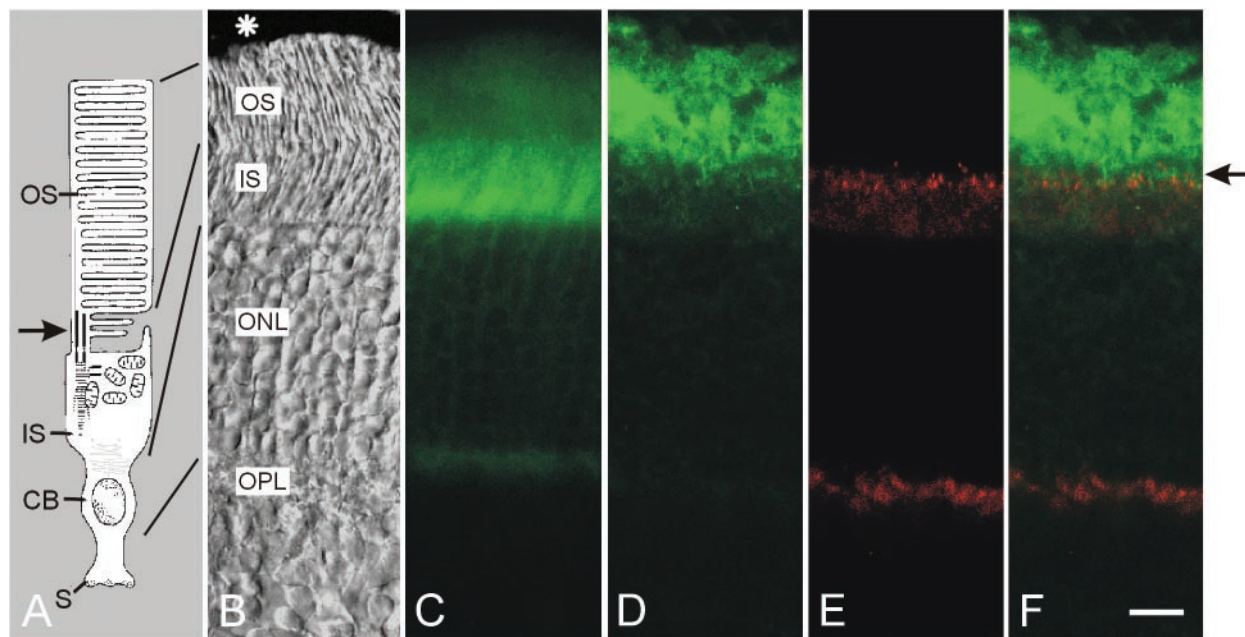


FIG. 1. Light-stimulated translocations of transducin in mouse retinas. (A) Schematic representation of a rod photoreceptor cell. Vertebrate photoreceptors are divided into distinct compartments: the photosensitive outer segment (OS), which contains stacks of hundreds of membrane disks, the place of visual transduction; the inner segment (IS), which contains the biosynthetic machinery of the cell, including the endoplasmic reticulum, the Golgi apparatus, and numerous mitochondria; the cell body (CB), which is localized in the outer nuclear layer (ONL in panel B) of the retina and contains the nucleus; and the synaptic terminal (S) in the outer plexiform layer (OPL in panel B) of the retina, which electrically connects the cell to downstream neurons of the retina. The arrow points to the nonmotile connecting cilium, which is the only cytoplasmic linkage between the OS and the IS. (B) Differential interference contrast image of a cryosection through a light-adapted mouse retina. The asterisk indicates retinal pigment epithelium. (C) Indirect anti- G_{α} immunofluorescence in the section through the light-adapted mouse retina pictured in panel B. Anti- G_{α} labeling is predominantly found in the IS of photoreceptor cells. Fade anti- G_{α} staining is present in the cytoplasm of cell bodies (ONL in panel B) and in the synaptic terminals (OPL in panel B) but also in the OS (see panels A and B) of photoreceptors. (D to F) Indirect double-immunofluorescence labeling of G_{α} and centrin in a cryosection through a dark-adapted mouse retina. (D) Anti- G_{α} immunofluorescence (Alexa 488) is predominantly found in the OS of photoreceptors. (E) Anti-centrin immunofluorescence (Alexa 546) is concentrated in the connecting cilium between the IS and OS of photoreceptors. (F) Merged images of D and E may indicate colocalization of G_{α} and centrin in the joint between photoreceptor IS and OS (arrow). Bar, 10 μ m.

that the Ca^{2+} -binding protein centrin 1 interacts specifically with the visual G-protein transducin in a Ca^{2+} -dependent manner. We demonstrate the colocalization of both proteins in the cilia. Based on the experimental data, we propose a model for centrin action, in which the G protein is freed for participation in the visual cascade localized at the disk membranes in the outer segment. The potential significance of such a mechanism results from the formation of a ciliary barrier and/or store for the G protein, which may provide a potential link between signal transduction and intracellular protein transport.

MATERIALS AND METHODS

Animals and tissue preparation. Adult Sprague-Dawley albino rats and C57BL/6J mice were maintained on a cycle of 12 h of light and 12 h of darkness, with food and water ad libitum. After sacrifice of the animals in CO_2 , entire eyeballs were dissected or retinas were removed through a slit in the cornea prior to further analysis. Bovine eyes were obtained from the local slaughterhouse.

Isolation of bovine ROS. Rod outer segments (ROS) were purified from fresh, dark-adapted bovine retinas using the discontinuous sucrose gradient method described in reference 39. Retinas were dissected and ROS were isolated under dim red illumination. All subsequent procedures were performed at 0 to 5°C, and the ROS were stored at $-80^{\circ}C$ prior to use.

Preparation of outer segment proteins. Rhodopsin was prepared by removing the soluble and membrane-associated proteins from the disk membrane by repetitive washes with a low-ionic-strength buffer (3). All purification steps were

performed under dim red illumination, and the membrane suspension was stored at $-80^{\circ}C$ until use. Phosphorylated rhodopsin was prepared as described (45). Transducin (G_{α} holo) was isolated from frozen dark-adapted bovine retinas according to the method of Heck and Hofmann (16). Subunits were further purified on blue Sepharose (1 ml of HiTrap Blue; Amersham Biosciences) at a flow rate of 3 ml/h. Protein eluted with starting buffer {20 mM 1,3-bis[tris(hydroxymethyl)-methylamino]propane (BTP), pH 7.5; 1 mM $MgCl_2$; 2 mM dithiothreitol (DTT)} contains inactive $\beta\gamma$ -subunit of transducin ($G_{\alpha}\beta\gamma$) (40). Active $G_{\alpha}\beta\gamma$ was eluted with a linear gradient of 0 to 0.3 M NaCl (15 ml). G_{α} was eluted with 1 M NaCl. The subunits were dialyzed against measuring buffer (20 mM BTP, pH 7.4; 130 mM NaCl; 5 mM $MgCl_2$; 2 mM DTT), concentrated (Amicon YM-10 device), and stored at $-40^{\circ}C$. Unphosphorylated rhodopsin kinase (RK) was purified as described previously (44), arrestin was purified from frozen dark-adapted bovine retinas (18), GCAP1 was generated as described previously (53), recoverin was purified as described previously (21), and calmodulin was purchased from Calbiochem (catalog no. 208694).

Centrin 1 expression. Mouse centrin 1 cDNA was kindly provided by Jeff L. Salisbury, Mayo Clinic Foundation, Rochester, Minn., and was cloned into the pGEX-4T3 expression vector (Amersham Biosciences) using *Bam*HI and *Eco*RI restriction sites. Expression and purification of the GST fusion protein was performed according to the manufacturer's instructions. After cleavage of the fusion protein with thrombin on the column, centrin was eluted in 20 mM BTP (pH 7.5)–130 mM NaCl–1 mM $MgCl_2$ and passed over a benzamide Sepharose 6B (Amersham Biosciences) column to remove thrombin.

Antibodies. The mouse monoclonal antibody (MAb) against frog G_{α} (clone 4A) was used. MAb 4A is well characterized and commonly used in other studies (e.g., see reference 32), also recognizing bovine G_{α} (57). Affinity-purified polyclonal rabbit antibodies against the anti- α - and anti- β -subunit of the G protein were obtained from Biomol Research Laboratories, Inc. (Plymouth Meeting,

Pa.). MAbs to arrestin (clone 3D1.2) were applied as previously characterized (36). MAb against centrin (clone 20H5) has been previously characterized (1). Affinity-purified polyclonal antisera from rabbit against algal centrin (MC1) (1) and against recombinantly expressed mouse centrin 1 (pMmC1) were applied (A. Gießl, A. Schmitt, and U. Wolfrum, unpublished data).

IP. Immunoprecipitation (IP) was performed in the presence and absence of Ca^{2+} . Isolated bovine retinas or photoreceptor fragments were lysed in pre-heated lysis buffer (10 mM Tris-HCl, pH 7.4; 150 mM NaCl; 10 mM NaF; 20 mM β -glycerophosphate; 1% sodium dodecyl sulfate [SDS]; 5% NP-40; 5% deoxycholic acid) with brief sonication. After centrifugation (10 min; $20,800 \times g$; 4°C) soluble proteins were diluted with 9 volumes of IP buffer HNTG (20 mM HEPES, pH 7.4; 150 mM NaCl; 1% Triton X-100; 10% glycerol) with or without 25 to 100 μM Ca^{2+} or with or without 1 mM EGTA, respectively, containing a protein inhibitor cocktail (phenylmethylsulfonyl fluoride, leupeptin, pepstatin A, and aprotinin). For IP antiserum, pMmC1 or monoclonal 20H5 was incubated with bovine serum albumin (BSA) (5%)–preadsorbed protein A- or protein A/G-Sepharose beads (Pierce), respectively, in HNTG for at least 2.5 h at 4°C prior to adding to the protein samples and incubation overnight at 4°C on a rocker. After washes in HNTG, the immunocomplexes were collected by centrifugation and analyzed by sodium dodecyl sulfate-polyacrylamide gel electrophoresis (SDS-PAGE) followed by Western blotting.

Western blot analyses and SDS-PAGE. For Western blots, isolated retinas or immunocomplexes obtained after IP were homogenized and placed in SDS-PAGE sample buffer (62.5 mM Tris-HCl, pH 6.8; 10% glycerol; 2% SDS; 5% mercaptoethanol; 1 mM EDTA; 0.025% bromophenol blue). Proteins were separated by SDS-PAGE (23), transferred electrophoretically to Immobilon-P, and probed with primary and secondary antibodies (59).

Centrifugation assay. The binding of the calcium-dependent mouse centrin 1 (MmCen1)- G_t complex to rhodopsin was determined using a centrifugation assay (18, 44). MmCen1 (5 μM), G_t (1 μM), and rhodopsin (5 μM) were incubated in 50 mM BTP, pH 7.0, containing 80 mM NaCl, 1 mM MgCl_2 , and either 1 μM CaCl_2 , 100 μM CaCl_2 , or 1 mM EGTA. Aliquots (80 μl) of these samples were illuminated with a 150-W fiber-optic light source filtered through a heat filter (Schott KG2) and a 495-nm long-pass filter for 10 min on ice and pelleted by ultracentrifugation (10 min; $208,000 \times g$; 4°C). After removal of the supernatant, the pellet was washed once (without resuspending, to avoid loss membrane bound proteins) with buffer and then resuspended in 80 μl of buffer. The amount of the MmCen1- G_t complex either bound to the membrane pellet or present in the supernatant was analyzed by densitometry on Coomassie blue-stained SDS-PAGE gels. All samples were heated to 95°C for 10 min in the presence of SDS, in order to aggregate most of the rhodopsin, which would otherwise mask the $G_t\beta\gamma$ -subunit.

Centrin blot overlay assay. For centrin overlay assay solubilized proteins of bovine retina were separated by SDS-PAGE and transferred to a polyvinylidene difluoride membrane. The nitrocellulose membrane was blocked for 16 h with 5% nonfat dry milk and 3% BSA in TBS (10 mM Tris-HCl, pH 7.4; 150 mM NaCl; 0.05% Tween 20) and for 1 h in Boehringer blocking solution. After being washed for 15 min in HNTG buffer (containing either 1 mM CaCl_2 or 6 mM EGTA) the membrane was incubated overnight in HNTG buffer containing either 1 mM CaCl_2 or 6 mM EGTA, 0.5% BSA, and recombinantly expressed MmCen1 (67 $\mu\text{g/ml}$). After being rinsed in TBS three times, the blot was air dried, rehydrated by brief immersion in methanol, and blocked with 5% nonfat dry milk in TBS and Boehringer blocking solution. Centrin-binding proteins were visualized by standard Western blot immunoanalysis using a MAb against centrin (clone 20H5).

Immunofluorescence microscopy. Eyes from light-adapted (8 h, ~ 300 lx) and dark-adapted (8 h) adult C57BL/6J mice were prefixed in 4% paraformaldehyde in phosphate-buffered saline (PBS) for 1 h at room temperature. Prefixed tissue was washed, infiltrated with 30% sucrose in PBS overnight, and cryofixed in melting isopentane and cryosectioned as described (58). Cryosections were placed on poly-L-lysine-precoated coverslips and incubated with 50 mM NH_4Cl and 0.1% Tween 20 in PBS. PBS-washed sections were blocked with blocking solution (0.5% cold water fish gelatin σ plus 0.1% ovalbumin σ in PBS) for 30 min, and then incubated with primary antibody in blocking solution overnight at 4°C . Washed sections were subsequently incubated with secondary antibodies conjugated to Alexa 488 or Alexa 546 (Molecular Probes) in blocking solution for 1 h at room temperature in the dark. After washing, sections were mounted in Mowiol 4.88 (Farbwerke Hoechst, Frankfurt, Germany), containing 2% *n*-propyl-gallate. In appropriate controls, in no case was a reaction observed in the controls. Mounted retinal sections were examined with a Leica DMRP microscope. Images were obtained with a Hamamatsu ORCA ER charge-coupled device camera (Hamamatsu) and processed with Adobe Photoshop (Adobe Systems Inc.).

Immunoelectron microscopy. Freshly isolated rat and mouse retinas were fixed and embedded in LR White as previously described (62). Ultrathin sections collected on Formvar-coated nickel grids were etched with saturated sodium periodate (Sigma) prior to immunogold labeling, as described in detail by Wolfrum and Schmitt (62). Nanogold labeling was carried out by the silver-enhanced method according to the method of Danscher (10). Counterstained sections were analyzed in Zeiss EM 900 or Leo EM906 electron microscope. Immunoelectron microscopic labelings of different ciliary domains of rat photoreceptor cells were quantified by counting silver-enhanced gold particles on electron microscopic micrographs or digitized images of ultrathin sections.

Determination of protein concentrations. The concentrations of rhodopsin and phosphorylated rhodopsin were determined spectrophotometrically at 498 nm (43). Expressed centrin 1 (MmCen1) concentration was determined using the Pierce bicinchoninic protein assay. The concentrations of purified transducin (G_t holo) and the subunits of transducin ($G_t\alpha$ and $G_t\beta\gamma$) were determined using the Bradford method (8). The amount of activable $G_t\alpha$ was measured precisely by fluorometric titration with guanosine 5'-3-*O*-(thio)triphosphate (13). Purified arrestin was determined spectrophotometrically at 278 nm, assuming a molar absorption coefficient, $E^{0.1\%}$, of 0.638 (45) and a molecular mass of 45,300 Da. The concentration of the RK was measured either spectrophotometrically at 278 nm assuming an absorption coefficient of $70,000 \text{ M}^{-1} \text{ cm}^{-1}$, or using the Bradford method.

Determination of free calcium. The free calcium concentration was set using an EGTA buffer system (50 mM BTP, pH 7.0; 80 mM NaCl; 5 mM MgCl_2 ; 50 μM EGTA). The original concentration in the saline buffer (typically 18 μM CaCl_2) was measured spectrophotometrically, using arsenazo III (64). After Ca^{2+} determination in the buffer and with the known addition of EGTA and Ca^{2+} , the actual concentration of free Ca^{2+} was calculated (52).

Size-exclusion chromatography. Size-exclusion chromatography was used to characterize the complex formation between MmCen1 and transducin and its subunits. To determine the binding of MmCen1 to transducin the molecular weight shift of the complex was used. MmCen1 (10 μg) and 10 μg of G_t holo (or G_t subunits: $G_t\alpha$ and $G_t\beta\gamma$) were incubated in 50 mM BTP, pH 7.0, containing 80 mM NaCl, 1 mM MgCl_2 , and either 100 μM CaCl_2 or 1 mM EGTA for 5 min at room temperature. As controls MmCen1, G_t , and G_t subunits were incubated alone. The reaction mixtures were loaded on a Superose TM 12 column (Amersham Biosciences) equilibrated with the same buffer, using the Smart System (flow rate, 40 $\mu\text{l/min}$; Amersham Biosciences). The elution was monitored by absorbance at 280 nm, and 40- μl fractions were collected for the subsequent SDS-PAGE analysis.

Kinetic light-scattering (KLS). Light-scattering changes were measured in a setup described in detail by Heck et al. (18). All measurements were performed in 10-mm path cuvettes with 300- μl volumes in 50 mM BTP, pH 7.0; 80 mM NaCl; 5 mM MgCl_2 ; and either 100 μM CaCl_2 or 1 mM EGTA at 20°C . Reactions were triggered by flash photolysis of rhodopsin with a green (500 ± 20 nm) flash, attenuated by appropriate neutral density filters. The flash intensity is quantified photometrically by the amount of rhodopsin bleached and expressed in the mole fraction of photoexcited rhodopsin ($R^*/R = 32\%$). The scattering signal is interpreted as a gain of protein mass bound to disk membranes and quantified as described (17, 18). Light-scattering binding signals were corrected by a reference signal (N signal) measured on a sample without added G_t holo as described by Pulvermüller et al. (44).

RESULTS

Light-stimulated translocation of transducin in retinas. To determine the distribution of transducin in light- and dark-adapted mouse retinas we probed cryosections through mouse eyes with indirect immunofluorescence of anti- $G_t\alpha$. Our experiments revealed that transducin was relocated when retinas were compared from light- and dark-adapted mouse retinas. In light-adapted retinas, $G_t\alpha$ was found predominantly in the inner segment of photoreceptor cells, the cytoplasm of the photoreceptor cell body (outer nuclear layer), and the synaptic terminal (Fig. 1B and C). In contrast to previous observations (41, 55), a fade anti- $G_t\alpha$ staining was also obvious in photoreceptor outer segments in light-adapted retinas (Fig. 1C). To determine whether other soluble proteins of the visual transduction cascade also distribute in dependence on different light

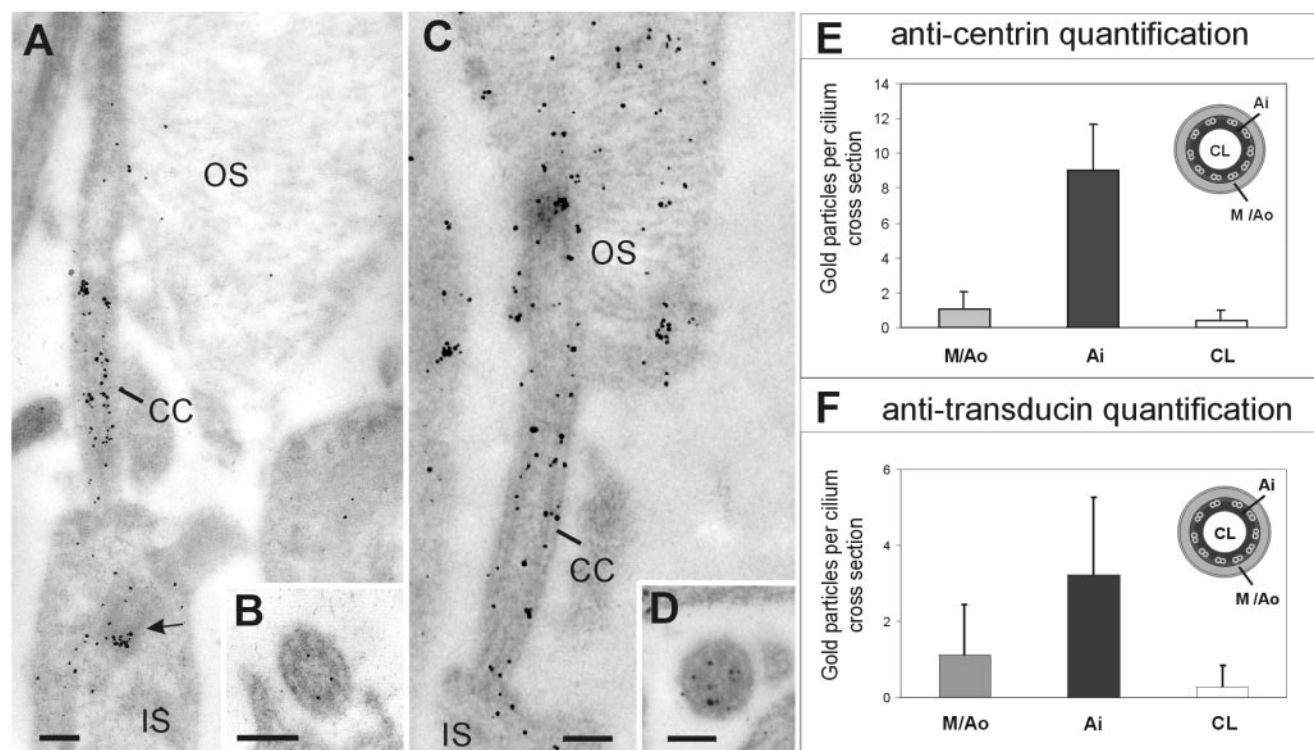


FIG. 2. Immunoelectron microscopic localization of centrin and G_{α} in the connecting cilium of rod photoreceptor cells. (A) Silver-enhanced immunogold labeling of centrin in a longitudinal section of parts of a rat rod photoreceptor cell. Centrin labeling is exclusively localized in the connecting cilium (CC) and the basal body complex (arrow) in the inner segment (IS) of photoreceptors. (B) A transverse section reveals that centrin is localized in the subcilial domain of the cilial lumen encircled by axonemal microtubule doublets. (C) Silver-enhanced immunogold labeling of G_{α} in a longitudinal section of parts of a dark-adapted rat rod photoreceptor cell. G_{α} labeling is most prominent in the outer segment (OS) of rod photoreceptors. However, G_{α} is also detected in the CC, where it is concentrated in the domain of the cilial lumen. (D) A transverse section reveals that G_{α} is also concentrated in the cilium in the central subcilial domain. (E) Silver-enhanced gold particle quantification of anticentrin immunolabeling in different subcilial domains of photoreceptor CC. The histogram indicates that centrin is significantly enriched at the inner face of the photoreceptor axoneme. (F) Silver-enhanced gold particle quantification of anti- G_{α} immunolabeling in different subcilial domains of photoreceptor CC. The histogram indicates mean numbers of gold particles per cilium transverse. G_{α} is concentrated at the inner face of the photoreceptor axoneme. Abbreviations for subcilial domains: Ai, axoneme inner face; CL, cilial lumen; M/Ao, membrane and axoneme outer face. Bars: 150 nm (A), 170 nm (B), 150 nm (C), and 120 nm (D). Error bars, standard deviations.

conditions, we immunostained arrestin (soluble photoreceptor-specific protein) in parallel cryosections through light- and dark-adapted mouse eyes. As expected from previous studies, arrestin was simultaneously translocated in response to light in the opposite direction (data not shown; see also references 29, 41, and 55). Present results on light-induced translocation of G_{α} are similar to the data previously reported on movements of G_{α} in rat retinas (55) and of G_{β} in BALB/cJ mouse retinas (41), indicating that the G_{α} is translocated in a manner dependent on light in vertebrate photoreceptor cells.

To determine whether transducin is translocated through the connecting cilium, the intracellular linkage between the photoreceptor inner and outer segments, we performed indirect double-immunofluorescence labeling of G_{α} and centrin, a cytoskeletal protein in the cilium of vertebrate photoreceptor cells (59, 60). We observed significant colocalization of both proteins in the joint between the inner and outer segments of photoreceptor cells (Fig. 1C to E).

Centrin and transducin colocalize in the cilium of rod photoreceptor cells. To determine the precise localization of centrin and transducin in the connecting cilium of photoreceptor

cells, we performed immunoelectron microscopy of centrin and G_{α} on ultrathin sections through mammalian retinas. In highly sensitive silver-enhanced Nanogold-labeling experiments, all antibodies to centrin used (polyclonal antibodies MC1 and pMmC1; MAb clone 20H5) showed the same labeling pattern, although the polyclonal antibodies MC1 and pMmC1 gave the strongest signal. Centrin was detected in the centrioles of centrosomes and basal bodies of all types of retinal cells and the connecting cilium in rod and cone photoreceptor cells in all vertebrates investigated (see also reference 59) (Fig. 2A and B). Although previous studies have revealed that none of the anticentrin antibodies discriminates between the centrin isoforms 1 (MmCen1) and 2 (MmCen2), the isoform detected in the photoreceptor cilium most probably resembles the centrin isoform MmCen1 (25, 60).

Immunoelectron microscopic analysis of dark-adapted retinas revealed that, as expected, the visual G-protein transducin was predominantly labeled by anti- G_{α} at the disk membranes of ROS where the signal transduction events take place, but abundant silver-enhanced gold particles were also localized in the metabolic active inner segment of all mammals investi-

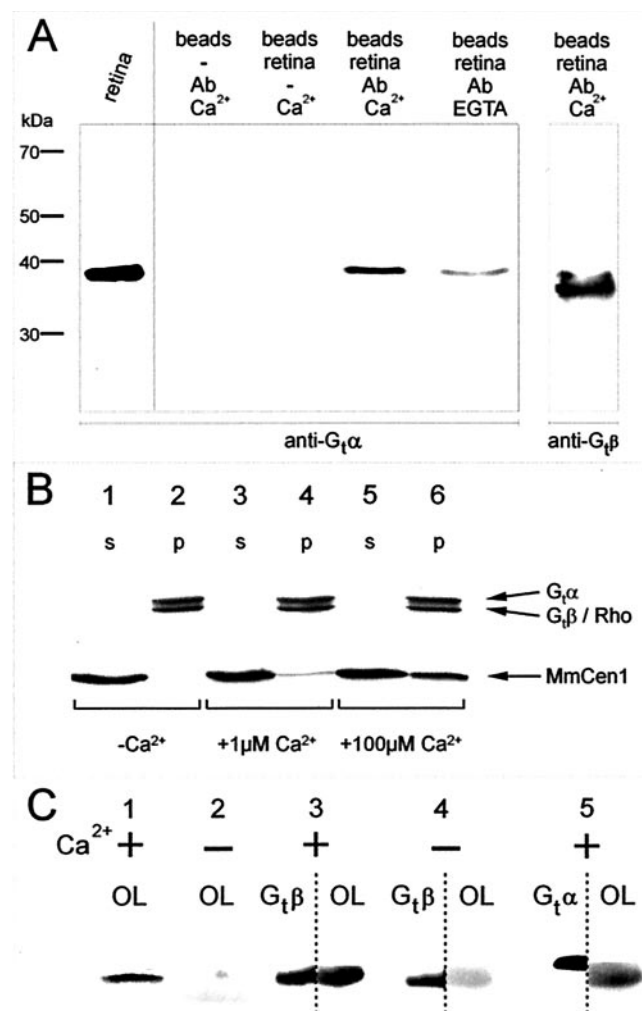


FIG. 3. Transducin binds in vitro to centrin in a calcium-dependent manner. (A) Coimmunoprecipitation of transducin with centrin from bovine retina lysates. Western blot analysis demonstrates that the mouse MAb to frog G_tα (clone 4A) detects G_tα as a 37-kDa protein band in lysate of bovine retina (first lane). The second through fifth lanes show Western blot analysis with anti-G_tα as follows (respectively): control precipitation without retina lysate, control precipitation without antibodies, IPs with MAb anticentrin (clone 20H5) in the presence of 25 μM calcium, and IPs with MAb anticentrin (clone 20H5) in the absence of calcium (1 mM EGTA). The last lane shows Western blot analysis with rabbit polyclonal anti-G_tβ of IP with polyclonal antibody anticentrin 1 (pMmC1). G_tα and G_tβ are coimmunoprecipitated from lysates of bovine retinas by anticentrin antibodies. (B) Membrane binding of the centrin-transducin complex. Centrifugation assay of the rhodopsin membrane binding of the calcium-dependent preformed MmCen1-transducin complex. Aliquots of membrane suspensions (5 μM) supplemented with 1 μM G_t and 5 μM MmCen1 in the presence of 1 mM EGTA (lanes 1 and 2), 1 μM CaCl₂ (lanes 3 and 4), and 100 μM CaCl₂ (lanes 5 and 6) were pelleted by centrifugation. The pellets (p) and supernatants (s) were analyzed by SDS-PAGE. For measuring conditions, see Material and Methods. (C) Analysis of centrin blot overlays with bovine retinal proteins. Shown is a Western blot of retinal proteins overlaid with recombinantly expressed MmCen1. Bound centrin was detected by immunolabeling with MAb against centrin. Lane 1 shows that in the presence of Ca²⁺ (1 mM CaCl₂), MmCen1 bound at 38 kDa to protein which appeared intensely labeled. Lane 2 shows that in the absence of Ca²⁺ (6 mM EGTA), MmCen1 binding was dramatically reduced. For specific determination of the centrin-binding protein, Western blotted lanes were cut in half and processed in parallel for immunolabeling

gated (Fig. 2C and D). Moreover, transducin was also detected in the connecting cilium linking both photoreceptor segments (Fig. 2C and D).

For quantification of the immunolabelings of centrin and G_tα in the connecting cilium, the number of silver-enhanced gold particles in different ciliary domains was determined in transverse sections through the connecting cilium of rat photoreceptor cells. Figure 2E shows that MmCen1 was predominantly detected at the inner surface of the microtubule doublets of the cilium. In other domains of the connecting cilium, the label was not above background levels. The quantification of transducin immunolabeling in 20 ciliary transversal sections is shown in Fig. 2F. It reveals that most of the anti-G_tα label was concentrated in the connecting cilium, namely, specifically in the ciliary domain of the inner lumen. Thus, the present results demonstrate that transducin and centrin colocalize in a subciliary compartment of the photoreceptor-connecting cilium.

Centrin-transducin interaction demonstrated by coimmunoprecipitation and centrifugation assay. The spatial colocalization of centrin and transducin obtained with the high resolution of immunoelectron microscopy suggests that both proteins may physically interact in photoreceptor-connecting cilia. In order to test possible assembly of both proteins we used two different detection methods: (i) coimmunoprecipitation (Fig. 3A) and (ii) centrifugation studies (Fig. 3B).

In IP assays, proteins of dark-adapted bovine photoreceptor fragments were immunoprecipitated with anticentrin antibodies in the presence of calcium (25 to 100 μM) and the absence of free calcium (1 mM EGTA). In the presence of calcium, G_tα and G_tβ were detected by Western blot analysis in the immunoprecipitates obtained with anticentrin MAb 20H5, but not in control experiments without antibodies (Fig. 3A). In the absence of calcium, the amount of coimmunoprecipitated transducin was drastically reduced (Fig. 3A). The second approach involved a centrifugation method (18, 44), which further confirmed that in the presence of calcium the preformed complex of transducin and centrin binds to rhodopsin in the disk membrane (Fig. 3B). In the absence of calcium, no complex formation was found, which is seen in a shift of G_t but not of MmCen1 to the membrane (Fig. 3B, lanes 1 and 2). Increasing the amount of calcium leads to a significant shift of G_t and MmCen1 to the membranes (Fig. 3B, lanes 2 to 6). Taken together, these results yield the first evidence that the visual G protein interacts with the cytoskeletal protein centrin in a calcium-dependent manner and may assemble into functional protein-protein complexes in photoreceptor cells.

Centrin blot overlay of retinal proteins. To test if centrin could bind directly to the visual G protein, centrin blot overlays were performed with proteins of the bovine retina. Western blots containing retinal proteins were incubated with recombinantly expressed MmCen1, and the proteins bound to centrin were identified by immunolabeling the blots with anticentrin

with subunit-specific antibodies against G_tβ (lanes 3 [with Ca²⁺] and 4 [without Ca²⁺]), and G_tα transducin (lane 5) and for overlays with recombinantly expressed MmCen1 (67 μg/ml) (OL). The 38-kDa centrin-binding protein identified by centrin overlays had the same mobility as the G_tβ subunit.

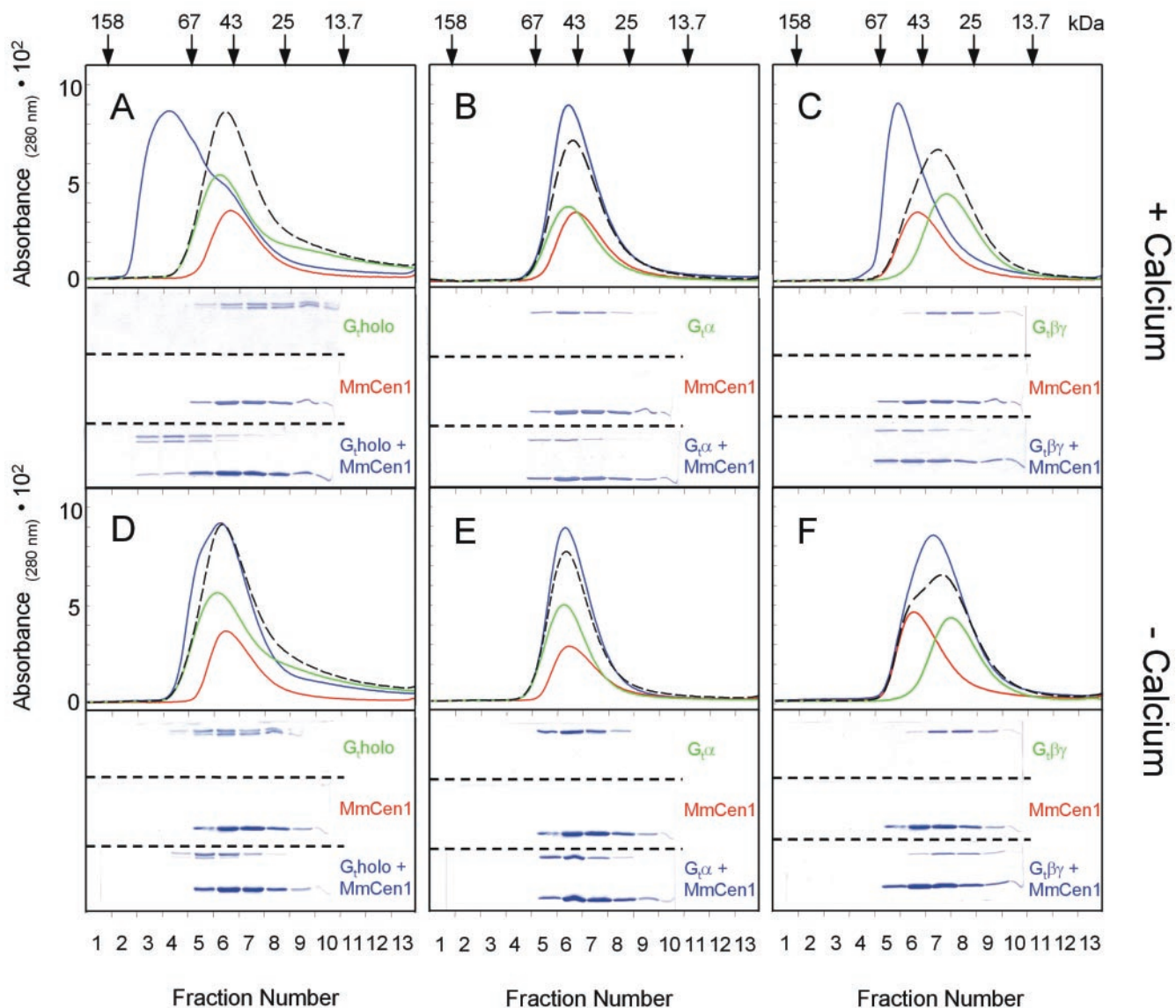


FIG. 4. Calcium-dependent interaction of MmCen1 with G_t and its subunits analyzed by size-exclusion chromatography and SDS-PAGE. (A to C) Elution profiles with 100 μ M $CaCl_2$ (upper panels) of MmCen1 alone (red), G_t or its subunits alone (green), and the mixture of MmCen1 with G_t or its subunits (blue). (D to F) Elution profiles with 1 mM EGTA, color-coded as indicated for panels A to C. The dotted lines are the calculated superpositions of the respective single component profiles (MmCen1 plus G_t or its subunits), yielding the predicted profiles for the mixture of the two noninteracting components. In the lower panel the SDS-PAGE analysis of the fractions of the size-exclusion chromatography is shown. Interactions of MmCen1 (10 μ g) with the transducin holoprotein (10 μ g) (A), with the $G_t\alpha$ -subunit (10 μ g) (B), and with the $G_t\beta\gamma$ -subunit (10 μ g) (C) in the presence of 100 μ M $CaCl_2$ are shown, as is interaction of MmCen1 with transducin and its subunits without calcium (1 mM EGTA) (D to F); G_t holoprotein elutes at an apparently lower molecular weight, compared to its subunits (6).

antibodies. These overlays revealed that centrin binding to retinal proteins was restricted to Ca^{2+} -activated centrin (Fig. 3C, lanes 1 and 2). Western blot analysis with subunit specific antibodies against $G\alpha$ and $G\beta$ showed that one of the identified centrin-binding proteins comigrated with the $G_t\alpha$ and $G_t\beta$ subunits of transducin at about 37 to 39 kDa (data not shown). For a more precise determination of the interacting G-protein subunit we dissected transblotted protein lanes and incubated them either with recombinantly expressed centrin or anti-G-protein antibodies. This analysis revealed the $G_t\beta$ subunit as

the identified 37-kDa centrin-binding protein (Fig. 3C, lanes 3 to 5).

Demonstration of centrin-transducin interaction by size-exclusion chromatography. The binding of purified transducin and its subunits ($G_t\alpha$ and $G_t\beta\gamma$) to MmCen1 was investigated in vitro using size-exclusion chromatography and SDS-PAGE-colorimetry. The elution profiles in Fig. 4A demonstrate the presence of a complex between MmCen1 and the transducin holoprotein G_t holo. In the presence of calcium (100 μ M $CaCl_2$), the elution peak of the MmCen1- G_t holo complex is

significantly shifted to higher molecular weights, compared to a theoretical peak, calculated for the superposition of the single-component profiles. The transducin subunits (G_{α} and $G_{\beta\gamma}$) interacted differently with MmCen1 in the presence of calcium. With G_{α} in its inactive, GDP-bound form (Fig. 4B), the elution peak is not shifted to any significant extent, compared to the calculated trace. The same applies to the permanently activated, 5'-3-*O*-(thio)triphosphate-bound G_{α} (data not shown). However, $G_{\beta\gamma}$ shows the shift to higher molecular weight characteristic of complex formation (Fig. 4C). In the absence of calcium (1 mM EGTA), no interaction with MmCen1 was found with $G_{\beta\text{holo}}$ or any of the G-protein subunits (Fig. 4D to F). The SDS-PAGE patterns in the lower part of each figure yield the additional information that both the G_{α} subunit and the $G_{\beta\gamma}$ complex are present in the complex with centrin, although G_{α} alone does not interact (compare Fig. 4A and B), confirming the results shown by overlay assays (Fig. 3C). Present size-exclusion chromatographies do not allow us to quantify the subunit composition (see for example the low apparent molecular weight of $G_{\beta\text{holo}}$ in the elution profile of Fig. 4A).

Properties of centrin-transducin interaction. The formation of stable complex between transducin and photoactivated rhodopsin in the absence of GTP can be readily assayed by the transition of soluble $G_{\beta\gamma}$ to the membrane via its effect on light scattering (binding signal) (see Materials and Methods and references 17 and 22). The assay is applicable to any soluble protein that interacts with Rho^* (18) and can also serve to analyze changes in the amount and/or molecular weight of transducin when it interacts with centrin. Addition of recombinantly expressed MmCen1 led to an enhanced amplitude of the binding signal in a Ca^{2+} -dependent manner (Fig. 5, inset). In the absence of free Ca^{2+} (1 mM EGTA), however, no significant difference with or without MmCen1 was observed (Fig. 5B). We interpret these data as a Ca^{2+} -dependent interaction of MmCen1 with soluble $G_{\beta\gamma}$.

The centrin titration curve (Fig. 5) is consistent with a model in which each $G_{\beta\text{holo}}$ binds a homooligomer ($n \geq 3$) of centrin, in agreement with the known tendency of centrins to form such small homooligomers (12). Excess of $G_{\beta\gamma}$ reverted the effect of centrin on the binding signal, as expected, because $G_{\beta\gamma}$ alone can bind centrin (see above) but not Rho^* (data not shown). The binding characteristics of MmCen1 were not significantly changed when the GST fusion remained at the centrin N terminus, indicating that the latter is not involved in the interaction with transducin (data not shown).

Calcium dependence of centrin-transducin interaction. When the binding signals are measured at a fixed concentration of centrin (and $G_{\beta\gamma}$) and the concentration of free Ca^{2+} is varied (Fig. 6), a fit to the data revealed a cooperativity of 1.7 ± 0.2 . MmCen1 exists (as other calcium-binding proteins like calmodulin, recoverin, guanylate cyclase-activating protein, etc.) in two states, namely, a Ca^{2+} -free form and one or several Ca^{2+} -binding forms (46, 51). Because the binding of $G_{\beta\gamma}$ to Rho^* in vitro does not depend on Ca^{2+} , we conclude that centrin binds to $G_{\beta\gamma}$ when two or more of its Ca^{2+} -binding sites are occupied. The 50% effective concentration (EC_{50}) for Ca^{2+} binding is $4.6 \mu\text{M}$ free Ca^{2+} (Fig. 6).

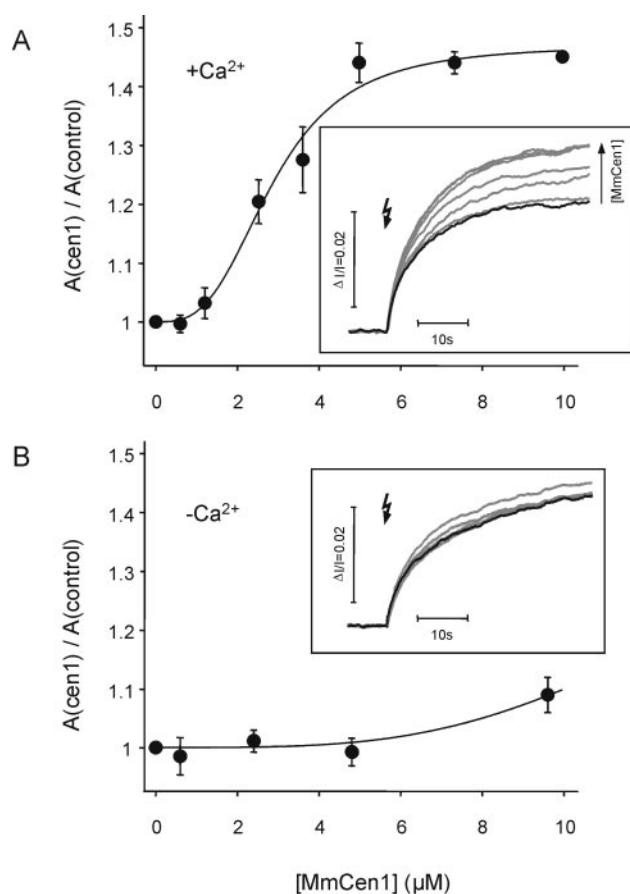


FIG. 5. Titration of KLS $G_{\beta\gamma}$ -binding signal with MmCen1. Shown is the dependence of the amplitude of flash-induced KLS $G_{\beta\gamma}$ -binding signals on MmCen1 in the presence of Ca^{2+} (A) or EGTA (B). (A) MmCen1-dependent enhancement of the $G_{\beta\gamma}$ -binding signals (A_{cen1}), normalized to the amplitude of the $G_{\beta\gamma}$ -binding signal without added MmCen1 (control), in the presence of $100 \mu\text{M}$ $CaCl_2$. Data points were fitted using the Hill equation: $f = (A \cdot [MmCen1]^n) / ([MmCen1]^n + EC_{50}^n) + 1$, where $A = 0.47 \pm 0.03$, $n = 3.1 \pm 0.7$, and $EC_{50} = 2.8 \pm 0.2 \mu\text{M}$ (where A is the maximum MmCen1-dependent enhancement of the $G_{\beta\gamma}$ -binding signal and n is the Hill coefficient). The inset shows KLS binding signals ($0.5 \mu\text{M}$ $G_{\beta\gamma}$, $3 \mu\text{M}$ rhodopsin) in the presence of $0 \mu\text{M}$ MmCen1 (control; black curve) and $0.6, 1.2, 2.5, 3.6, 5, 7.3,$ and $10 \mu\text{M}$ MmCen1 (gray curves), respectively. (B) Same as panel A, but with 1 mM EGTA instead of $CaCl_2$. The inset shows KLS binding signals ($0.5 \mu\text{M}$ $G_{\beta\gamma}$, $3 \mu\text{M}$ rhodopsin) in the presence of $0 \mu\text{M}$ MmCen1 (control; black curve) and $0.6, 2.4, 4.8,$ and $9.6 \mu\text{M}$ MmCen1 (gray curves), respectively. Measuring conditions were as described in Materials and Methods. The error bars display the standard deviations ($n = 3$).

DISCUSSION

We report here the first identification of a calcium-induced interaction of a heterotrimeric G protein with a calcium-binding protein. The specialized morphology of the rod cell and the physicochemical properties of its light-sensitive disk membranes provided the immunocytochemical and biophysical tools to explore both the intracellular colocalization of the proteins and to quantify their interaction in vitro. We find that transducin, the heterotrimeric G protein of the visual transduction cascade, interacts with MmCen1, a member of the EF-hand superfamily of Ca^{2+} -binding proteins, in a strictly

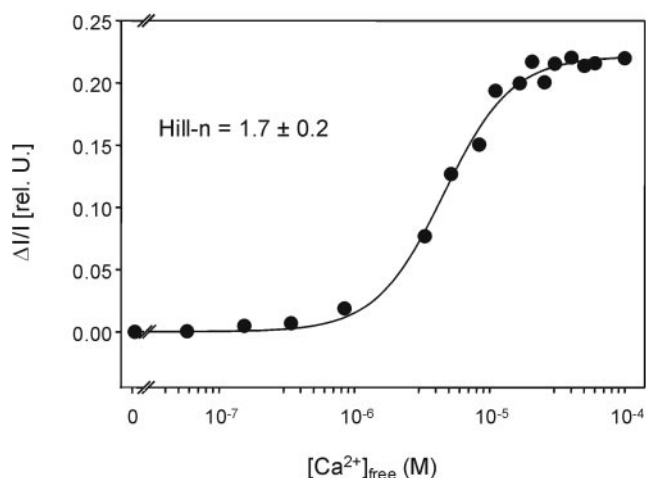


FIG. 6. Effect of calcium on the MmCen1-dependent enhancement of the G_t -binding signal. Shown are the amplitudes of KLS G_t -binding signals ($0.5 \mu\text{M } G_t$, $3 \mu\text{M}$ rhodopsin, $5 \mu\text{M}$ MmCen1) as a function of free Ca^{2+} concentration in solution (calculated as described in Materials and Methods). Data points were fitted using the Hill equation: $f = (A \cdot [\text{Ca}^{2+}]^n) / ([\text{Ca}^{2+}]^n + \text{EC}_{50}^n)$, where $A = 0.22 \pm 0.004$, $n = 1.7 \pm 0.2$, and $\text{EC}_{50} = 4.6 \pm 0.2 \mu\text{M}$ (see description of parameters in the legend to Fig. 5).

Ca^{2+} -dependent manner. Ca^{2+} -dependent regulation of signal transduction at the level of the G protein was previously suggested (24). However, the concentrated localization of centrin in the cilium but not in the outer segment excludes centrin-transducin interaction from a participation in the disk membrane bound processes. Our data rather suggest that centrin in a defined ciliary compartment of the photoreceptor cell regulates the supply of the G protein for signal transduction.

Ca^{2+} -induced assembly of centrin-transducin complex. Present light-scattering experiments demonstrate that the interaction between centrin and transducin is highly specific: on the one hand, the closest relative of centrin in the parvalbumin protein family, calmodulin, binds 10 to 15 times weaker, and the photoreceptor specific Ca^{2+} -binding proteins recoverin and guanylate cyclase-activating protein 1 do not show any detectable Ca^{2+} -dependent interaction with transducin (data not shown). On the other hand, MmCen1 does not bind to any other protein of the visual transduction cascade tested, e.g., arrestin, RK, or the visual pigment rhodopsin, nor does it influence the activity of the effector, cGMP phosphodiesterase (data not shown in this study).

Our data obtained by IP and centrifugation assays further confirm that MmCen1 binds to transducin in a Ca^{2+} -dependent manner. The Hill coefficient of 1.7 of this interaction indicates that each MmCen1 functional unit binds (at least) two Ca^{2+} ions. This is in agreement with data previously obtained by sequence analyses of mammalian centrin isoforms (including MmCen1), which have indicated that only two of the four putative EF hands remain functional for binding of Ca^{2+} (46, 63). Circular dichroism spectroscopy has previously shown that Ca^{2+} binding to centrin induces conformational changes in the protein (46, 56) which shift centrin into an activated state (46, 51). This activation is responsible for the contraction of centrin fibers in green algae (20, 47, 49, 50). It is also

suggested that Ca^{2+} -modulated centrin-based motility is also involved in Ca^{2+} -dependent structural changes at the mammalian centrosome, namely, in the centrosomal lattice (2, 15, 48). Ca^{2+} activation of centrins also increases their affinity to the cell division control protein Kar1p, a centrin target protein in yeast (15). In *Saccharomyces cerevisiae*, binding of cdc31p (cell division control protein 31, yeast centrin) to the spindle pole body protein Kar1p is part of a signal transduction cascade and leads to spindle pole body duplication. Here we show for the first time that Ca^{2+} -induced activation of MmCen1 is also relevant for the interaction with a heterotrimeric G protein, G_t .

The present data also demonstrate which of the G_t subunits contribute to the interaction. The α -subunit alone (in both its active GTP-bound and inactive GDP-bound forms) does not interact with centrin. In the presence of calcium, our size exclusion chromatography data reveal that $G_t\beta\gamma$ interacts with centrin as the isolated heterodimer or in the complex with the α -subunit. Present centrin overlay assays provide striking evidence that the G_t holo binds the centrin via a binding site at $G_t\beta$ and without affecting the interaction with $G_t\alpha$. This excludes $G_t\alpha$ interaction sites on $G_t\beta$ (7) as sites of interaction with centrin.

Furthermore, the conformational change in $G_t\alpha$ that accompanies the GTPase function of G_t is not affected by the interaction between centrin and $G_t\beta\gamma$. This was shown by studying the intrinsic fluorescence change (for methods, see reference 13) that monitors this reaction (data not shown).

G_t and centrin colocalize in a subdomain of the photoreceptor cilium. The visual G protein, as an essential component of the visual transduction cascade, is abundantly present at the disk membrane of the photoreceptor outer segment. Studies by Deretic and coworkers have previously indicated that, after de novo synthesis in the proximal inner segment, G_t subunits are cotransported with opsin-bearing membrane vesicles to the apical membrane at the base of the connecting cilium (11, 35). To our knowledge, the present immunoelectron microscopic detection is the first subcellular localization of $G_t\alpha$ —and thus presumably of the G_t holoprotein—in the cilium. It indicates that newly synthesized G_t is transferred via the connecting cilium to its final destination in the cytoplasmic compartment of photoreceptor outer segment. Our immunocytochemical studies further demonstrate that G_t is colocalized with centrin, which has previously been identified as a component of the ciliary cytoskeleton of photoreceptor cells (59, 60). Both proteins were found in the subciliary domain of the connecting cilium attached to the inner face of the axonemal microtubule-doublet ring. Since colocalization of G_t with centrin is restricted to this well-defined ciliary domain in mammalian photoreceptor cells, G_t and centrin presumably assemble the Ca^{2+} -dependent complex that arises from the in vitro analyses, in the connecting cilium.

Putative role of the centrin- G_t complex in mammalian photoreceptor cells. Any newly synthesized outer segment protein must be transported from the inner to the outer segment through the connecting cilium. This, however, is not the only function of this structure; it must also serve as a barrier against diffusion between inner and outer segments (5, 54). For example, in healthy cone and rod photoreceptor cells, the integral membrane protein opsin is highly concentrated in outer seg-

ment membranes and is present in low density in the inner segment membrane. The specialized cytoskeleton-membrane assemblage of the connecting cilium may play a critical, probably active role in preventing opsin from rediffusing to the inner segment under all physiological conditions (5, 28). In contrast to the unidirectional ciliary transport of membrane proteins, there is substantial evidence from previous work that the subcellular movement of soluble proteins between the inner and the outer segment occurs in both ways (5). Present and previously published experimental data (41, 55) demonstrate that a rapid exchange of $G_t\alpha$ and $G_t\beta$, as well as arrestin, between the inner and the outer segment is modulated by light: in the dark, G_t is highly concentrated in outer segments, while in the light, the majority of G_t is translocated and abundantly localized in the inner segment and the cell body of photoreceptor cells. In contrast, the distribution of arrestin under different light conditions is exactly the reverse (41, 55). These data are in agreement with recently obtained results indicating that the transport of arrestin and transducin through the connecting cilium occurs through different pathways (30). The remove of KIF3A, a subunit of the microtubule-based heterotrimeric molecular motor kinesin II, by Cre-loxP mutagenesis, does not alter G_t localization but causes misaccumulation of arrestin in mutated photoreceptor cells. This indicates that arrestin is probably transported by kinesin II in membrane-associated rafts. However, our immunoelectron microscopic results discussed above indicate that G_t is translocated in a different ciliary domain through the center of the photoreceptor cilium.

The dependence on light of transport phenomena supports the idea that the exchange of soluble proteins at the ciliary junction between the outer and inner segment is regulated by a light-modulated second messenger. A second messenger which dramatically changes with light conditions is Ca^{2+} . Changes of free Ca^{2+} reported in the literature (34) include the well-studied Ca^{2+} drop within the operating (single-quantum-detective) range of the rod and recent observations of Ca^{2+} increase in bright light (rod-saturated conditions) (31). Under the former condition, free Ca^{2+} in the rod cytoplasm is known to vary from 30 nM in the light to 500 to 700 nM in the dark (for a review, see Palczewski et al. [38]). Any change of the free Ca^{2+} in the outer segment should cause Ca^{2+} diffusion into the slender and short ciliary domain (in mammalian photoreceptors, the cilium measures $\sim 1 \mu\text{m}$ in length and the inner diameter of the axoneme is smaller than 80 nm) and induce Ca^{2+} activation of MmCen1. As a consequence, activated MmCen1 will bind with high affinity the G_t passing the ciliary lumen and may contribute to a Ca^{2+} -induced barrier for G_t in the connecting cilium, at the joint between the photoreceptor inner and outer segment. A drop of Ca^{2+} should induce the disassembly of the MmCen1- G_t complex, thus providing a necessary condition for the exchange of G_t between the inner and the outer segment of photoreceptor cells (41, 55). The Ca^{2+} -dependent assembly of a G protein with centrin, demonstrated here, is a novel aspect of the supply of signaling proteins in sensory cells and a potential link between molecular translocations and signal transduction in general.

ACKNOWLEDGMENTS

This work was supported by grants from the Deutsche Forschungsgemeinschaft (SSP 1025 Molecular Sensory Physiology, to A.P., O.P.E., K.P.H. [Ho832/6], and U.W. [Wo548/3]), the Fonds der Chemischen Industrie (to K.P.H.), and the FAUN-Stiftung, Nürnberg, Germany (to U.W.).

We are most grateful to H. E. Hamm, Institute for Neuroscience, Northwestern University, Chicago, Ill., for kindly supplying the MAB to frog α -transducin and to J. L. Salisbury, Mayo Clinic Foundation, Rochester, Minn., for providing us the mouse centrin 1 cDNA and antibodies raised against alga centrin. We thank E. Hessel for calcium determinations and R. Hauer, I. Semjonow, K. Lotz, E. Sehn, and K. Kubicki for skillful technical assistance.

REFERENCES

1. Baron, A. T., T. M. Greenwood, C. W. Bazinet, and J. L. Salisbury. 1992. Centrin is a component of the pericentriolar lattice. *Biol. Cell.* **76**:383–388.
2. Baron, A. T., V. J. Suman, E. Nemeth, and J. L. Salisbury. 1994. The pericentriolar lattice of PtK2 cells exhibits temperature and calcium-modulated behavior. *J. Cell Sci.* **107**:2993–3003.
3. Bauer, P. J. 1988. Evidence for two functionally different membrane fractions in bovine retinal rod outer segments. *J. Physiol.* **401**:309–327.
4. Bershadsky, A. D., and J. M. Vasiliev. 1988. Cytoskeleton. Plenum Press, New York, N.Y.
5. Besharse, J. C., and C. J. Horst. 1990. The photoreceptor connecting cilium: a model for the transition zone, p. 389–417. *In* R. A. Bloodgood (ed.), Ciliary and flagellar membranes. Plenum Press, New York, N.Y.
6. Bigay, J., E. Faurobert, M. Franco, and M. Chabre. 1994. Roles of lipid modifications of transducin subunits in their GDP-dependent association and membrane binding. *Biochemistry* **33**:14081–14090.
7. Bohm, A., R. Gaudet, and P. B. Sigler. 1997. Structural aspects of heterotrimeric G-protein signaling. *Curr. Opin. Biotechnol.* **8**:480–487.
8. Bradford, M. M. 1976. A rapid and sensitive method for the quantitation of microgram quantities of protein utilizing the principle of protein-dye binding. *Anal. Biochem.* **72**:248–254.
9. Brann, M. R., and L. V. Cohen. 1987. Diurnal expression of transducin mRNA and translocation of transducin in rods of rat retina. *Science* **235**:585–587.
10. Danscher, G. 1981. Localization of gold in biological tissue. A photochemical method for light and electron microscopy. *Histochemistry* **71**:81–88.
11. Deretic, D., and D. S. Papermaster. 1991. Polarized sorting of rhodopsin on post-Golgi membranes in frog retinal photoreceptor cells. *J. Cell Biol.* **113**:1281–1293.
12. Durussel, I., Y. Blouquit, S. Middendorp, C. T. Craescu, and J. A. Cox. 2000. Cation- and peptide-binding properties of human centrin 2. *FEBS Lett.* **472**:208–212.
13. Ernst, O. P., C. Bieri, H. Vogel, and K. P. Hofmann. 2000. Intrinsic biophysical monitors of transducin activation: fluorescence, UV-visible spectroscopy, light scattering, and evanescent field techniques. *Methods Enzymol.* **315**:471–489.
14. Errabolu, R., M. A. Sanders, and J. L. Salisbury. 1994. Cloning of a cDNA encoding human centrin, an EF-hand protein of centrosomes and mitotic spindle poles. *J. Cell Sci.* **107**:9–16.
15. Geier, B. M., H. Wiech, and E. Schiebel. 1996. Binding of centrins and yeast calmodulin to synthetic peptides corresponding to binding sites in the spindle pole body components Kar1p and Spc110p. *J. Biol. Chem.* **271**:28366–28374.
16. Heck, M., and K. P. Hofmann. 1993. G-protein-effector coupling: a real-time light-scattering assay for transducin-phosphodiesterase interaction. *Biochemistry* **32**:8220–8227.
17. Heck, M., and K. P. Hofmann. 2001. Maximal rate and nucleotide dependence of rhodopsin catalyzed transducin activation: initial rate analysis based on a double displacement mechanism. *J. Biol. Chem.* **276**:10000–10009.
18. Heck, M., A. Pulvermüller, and K. P. Hofmann. 2000. Light scattering methods to monitor interactions between rhodopsin-containing membranes and soluble proteins. *Methods Enzymol.* **315**:329–347.
19. Hofmann, K. P., and M. Heck. 1996. Light-induced protein-protein interactions on the rod photoreceptor disc membrane, p. 141–198. *In* A. G. Lee (ed.), Biomembranes II. JAI Press, Greenwich, Conn.
20. Huang, B., A. Mengersen, and V. D. Lee. 1988. Molecular cloning of cDNA for caltractin, a basal body-associated Ca^{2+} -binding protein: homology in its protein sequence with calmodulin and the yeast CDC31 gene product. *J. Cell Biol.* **107**:133–140.
21. Hughes, R. E., P. S. Brzovic, R. E. Klevit, and J. B. Hurley. 1995. Calcium-dependent solvation of the myristoyl group of recoverin. *Biochemistry* **34**:11410–11416.
22. Kühn, H., N. Bennett, M. M. Villaz, and M. Chabre. 1981. Interactions between photoexcited rhodopsin and GTP-binding protein: kinetic and stoichiometric analyses from light-scattering changes. *Proc. Natl. Acad. Sci. USA* **78**:6873–6877.

23. Laemmli, U. K. 1970. Cleavage of structural proteins during the assembly of the head of bacteriophage T4. *Nature* **227**:680–685.
24. Lagnado, L., and D. A. Baylor. 1994. Calcium controls light-triggered formation of catalytically active rhodopsin. *Nature* **367**:273–277.
25. Laoukili, J., E. Perret, S. Middendorp, O. Houcine, C. Guennou, F. Marano, M. Bornens, and F. Tournier. 2000. Differential expression and cellular distribution of centrin isoforms during human ciliated cell differentiation in vitro. *J. Cell Sci.* **113**:1355–1364.
26. Lee, V. D., and B. Huang. 1993. Molecular cloning and centrosomal localization of human caltractin. *Proc. Natl. Acad. Sci. USA* **90**:11039–11043.
27. Liu, X., I. P. Udovichenko, S. D. Brown, K. P. Steel, and D. S. Williams. 1999. Myosin VIIa participates in opsin transport through the photoreceptor cilium. *J. Neurosci.* **19**:6267–6274.
28. Liu, X., G. Vansant, I. P. Udovichenko, U. Wolfrum, and D. S. Williams. 1997. Myosin VIIa, the product of the Usher 1B syndrome gene, is concentrated in the connecting cilia of photoreceptor cells. *Cell Motil. Cytoskeleton* **37**:240–252.
29. Mangini, N. J., and D. R. Pepperberg. 1988. Immunolocalization of 48K in rod photoreceptors. Light and ATP increase OS labeling. *Investig. Ophthalmol. Vis. Sci.* **29**:1221–1234.
30. Marszalek, J. R., X. Liu, E. A. Roberts, D. Chui, J. D. Marth, D. S. Williams, and L. S. Goldstein. 2000. Genetic evidence for selective transport of opsin and arrestin by kinesin-II in mammalian photoreceptors. *Cell* **102**:175–187.
31. Matthews, H. R., and G. L. Fain. 2001. A light-dependent increase in free Ca²⁺ concentration in the salamander rod outer segment. *J. Physiol.* **532**:305–321.
32. Mazzoni, M. R., and H. E. Hamm. 1989. Effect of monoclonal antibody binding on alpha-beta gamma subunit interactions in the rod outer segment G protein, Gt. *Biochemistry* **28**:9873–9880.
33. Middendorp, S., A. Paoletti, E. Schiebel, and M. Bornens. 1997. Identification of a new mammalian centrin gene, more closely related to *Saccharomyces cerevisiae* CDC31 gene. *Proc. Natl. Acad. Sci. USA* **94**:9141–9146.
34. Molday, R. S., and U. B. Kaupp. 2000. Ion channels of vertebrate photoreceptors, p. 143–182. *In* D. G. Stavenga, W. J. DeGrip, and E. N. Pugh, Jr. (ed.), *Molecular mechanism in visual transduction*. Elsevier Science Publishers B.V., Amsterdam, The Netherlands.
35. Morel, V., R. Poschet, V. Traverso, and D. Deretic. 2000. Towards the proteome of the rhodopsin-bearing post-Golgi compartment of retinal photoreceptor cells. *Electrophoresis* **21**:3460–3469.
36. Nork, T. M., N. J. Mangini, and L. L. Millecchia. 1993. Rods and cones contain antigenically distinctive S-antigens. *Investig. Ophthalmol. Vis. Sci.* **34**:2918–2925.
37. Okada, T., O. P. Ernst, K. Palczewski, and K. P. Hofmann. 2001. Activation of rhodopsin: new insights from structural and biochemical studies. *Trends Biochem. Sci.* **26**:318–324.
38. Palczewski, K., A. S. Polans, W. Baehr, and J. B. Ames. 2000. Ca²⁺-binding proteins in the retina: structure, function, and the etiology of human visual diseases. *BioEssays* **22**:337–350.
39. Papermaster, D. S. 1982. Preparation of retinal rod outer segments. *Methods Enzymol.* **81**:48–52.
40. Parish, C. A., and R. R. Rando. 1994. Functional significance of G protein carboxymethylation. *Biochemistry* **33**:9986–9991.
41. Philp, N. J., W. Chang, and K. Long. 1987. Light-stimulated protein movement in rod photoreceptor cells of the rat retina. *FEBS Lett.* **225**:127–132.
42. Pugh, E. N., Jr., and T. Lamb. 2000. Phototransduction in vertebrate rods and cones: Molecular mechanism of amplification, recovery and light adaptation, p. 183–255. *In* D. G. Stavenga, W. J. DeGrip, and E. N. Pugh, Jr. (ed.), *Molecular mechanism in visual transduction*. Elsevier Science Publishers B. V., Amsterdam, The Netherlands.
43. Pulvermüller, A., D. Maretzki, M. Rudnicka Nawrot, W. C. Smith, K. Palczewski, and K. P. Hofmann. 1997. Functional differences in the interaction of arrestin and its splice variant, p44, with rhodopsin. *Biochemistry* **36**:9253–9260.
44. Pulvermüller, A., K. Palczewski, and K. P. Hofmann. 1993. Interaction between photoactivated rhodopsin and its kinase: stability and kinetics of complex formation. *Biochemistry* **32**:14082–14088.
45. Pulvermüller, A., K. Schröder, T. Fischer, and K. P. Hofmann. 2000. Interaction of metarhodopsin II: arrestin peptides compete with arrestin and transducin. *J. Biol. Chem.* **275**:37679–37685.
46. Salisbury, J. L. 1995. Centrin, centrosomes, and mitotic spindle poles. *Curr. Opin. Cell Biol.* **7**:39–45.
47. Salisbury, J. L., A. Baron, B. Surek, and M. Melkonian. 1984. Striated flagellar roots: isolation and partial characterization of a calcium-modulated contractile organelle. *J. Cell Biol.* **99**:962–970.
48. Salisbury, J. L., A. T. Baron, D. E. Coling, V. E. Martindale, and M. A. Sanders. 1986. Calcium-modulated contractile proteins associated with the eucaryotic centrosome. *Cell Motil. Cytoskeleton* **6**:193–197.
49. Salisbury, J. L., and G. L. Floyd. 1978. Calcium-induced contraction of the rhizoplast of a quadriflagellate green algae. *Science* **202**:975–976.
50. Sanders, M. A., and J. L. Salisbury. 1994. Centrin plays an essential role in microtubule severing during flagellar excision in *Chlamydomonas reinhardtii*. *J. Cell Biol.* **124**:795–805.
51. Schiebel, E., and M. Bornens. 1995. In search of a function for centrin. *Trends Cell Biol.* **5**:197–201.
52. Schoenmakers, T. J., G. J. Visser, G. Flik, and A. P. Theuvsenet. 1992. CHELATOR: an improved method for computing metal ion concentrations in physiological solutions. *BioTechniques* **12**:870–879.
53. Sokal, I., A. E. Otto Bruc, I. Surgucheva, C. L. Verlinde, C. K. Wang, W. Baehr, and K. Palczewski. 1999. Conformational changes in guanylyl cyclase-activating protein 1 (GCAP1) and its tryptophan mutants as a function of calcium concentration. *J. Biol. Chem.* **274**:19829–19837.
54. Spencer, M., P. B. Detwiler, and A. H. Bunt-Milam. 1988. Distribution of membrane proteins in mechanically dissociated retinal rods. *Investig. Ophthalmol. Vis. Sci.* **29**:1012–1020.
55. Whelan, J. P., and J. F. McGinnis. 1988. Light-dependent subcellular movement of photoreceptor proteins. *J. Neurosci. Res.* **20**:263–270.
56. Wiech, H., B. M. Geier, T. Paschke, A. Spang, K. Grein, J. Steinkotter, M. Melkonian, and E. Schiebel. 1996. Characterization of green algae, yeast, and human centrin. Specific subdomain features determine functional diversity. *J. Biol. Chem.* **271**:22453–22461.
57. Witt, P. L., H. E. Hamm, and M. D. Bownds. 1984. Preparation and characterization of monoclonal antibodies to several frog rod outer segment proteins. *J. Gen. Physiol.* **84**:251–263.
58. Wolfrum, U. 1991. Centrin- and alpha-actinin-like immunoreactivity in the ciliary rootlets of insect sensilla. *Cell Tissue Res.* **266**:231–238.
59. Wolfrum, U. 1995. Centrin in the photoreceptor cells of mammalian retinae. *Cell Motil. Cytoskeleton* **32**:55–64.
60. Wolfrum, U., and J. L. Salisbury. 1998. Expression of centrin isoforms in the mammalian retina. *Exp. Cell Res.* **242**:10–17.
61. Wolfrum, U., and A. Schmitt. 1999. Evidence for myosin VII driven rhodopsin transport in the plasma membrane of the photoreceptor connecting cilium, p. 3–14. *In* J. G. Hollyfield, R. E. Andersson, and M. LaVail (ed.), *Retinal degeneration diseases and experimental therapy*. Plenum Press, New York, N.Y.
62. Wolfrum, U., and A. Schmitt. 2000. Rhodopsin transport in the membrane of the connecting cilium of mammalian photoreceptor cells. *Cell Motil. Cytoskeleton* **46**:95–107.
63. Wottrich, R. 1998. Klonierung und computergeschützte Strukturanalyse von Centrinisoformen der Ratte (*Rattus norvegicus*). Master's thesis. Universität Karlsruhe, Karlsruhe, Germany.
64. Yingt, D. R., and J. F. Hoffman. 1983. Intracellular free Ca and Mg of human red blood cell ghosts measured with entrapped arsenazo III. *Anal. Biochem.* **132**:431–448.